2013

Investigation of trapping process in "Centrifuge-on-a-chip"

Jun Zhang
University of Wollongong, jz218@uowmail.edu.au

Ming Li
University Of Wollongong, ml433@uowmail.edu.au

Weihua Li
University of Wollongong, weihuali@uow.edu.au

Gursel Alici
University of Wollongong, gursel@uow.edu.au

Publication Details

Zhang, J., Li, M., Li, W. & Alici, G. (2013). Investigation of trapping process in "Centrifuge-on-a-chip". 2013 IEEE/ASME International Conference on Advanced Intelligent Mechatronics (AIM) (pp. 1266-1271). United States: IEEE.

Investigation of trapping process in "Centrifuge-on-a-chip"

Abstract
"Centrifuge-on-a-chip" is a versatile and multifunctional microfluidic chip which can conduct operations of selective trapping, enrichment, labeling and solution exchange. In this work, the mechanism of selective trapping ability was studied by both the experiments and numerical simulation. We proved the existence of shear gradient lift force in the expansion-contraction cavity and derived an explicit expression of it. Also, a numerical modeling was developed to study the trapping process of micro-particles in a "Centrifuge-on-a-chip". The effects of flow condition and particle size on the trapping process were investigated. It demonstrates that the derived expression and developed model are suitable for the prediction of particles' trapping process, which can assist the design of "Centrifuge-on-a-chip".

Keywords
trapping, process, centrifuge, chip, investigation

Disciplines
Engineering | Science and Technology Studies

Publication Details
Zhang, J., Li, M., Li, W. & Alici, G. (2013). Investigation of trapping process in "Centrifuge-on-a-chip". 2013 IEEE/ASME International Conference on Advanced Intelligent Mechatronics (AIM) (pp. 1266-1271). United States: IEEE.

Investigation of Trapping Process in "Centrifuge-on-a-chip"

Jun Zhang, Ming Li. Weihua Li*, and Gursel Alici

Abstract—**"Centrifuge-on-a-chip" is a versatile and multifunctional microfluidic chip which can conduct operations of selective trapping, enrichment, labeling and solution exchange. In this work, the mechanism of selective trapping ability was studied by both the experiments and numerical simulation. We proved the existence of shear gradient lift force in the expansion-contraction cavity and derived an explicit expression of it. Also, a numerical modeling was developed to study the trapping process of micro-particles in a "Centrifuge-on-a-chip". The effects of flow condition and particle size on the trapping process were investigated. It demonstrates that the derived expression and developed model are suitable for the prediction of particles' trapping process, which can assist the design of "Centrifuge-on-a-chip".**

I. INTRODUCTION

"Centrifuge-on-a-chip" is one kind of inertial microfluidics which employs the inertial migration of particles in the suddenly expanding area of micro-channel and trapping ability of micro-vortex. Compared to the standard commercial benchtop centrifuge, which is widely used in the cell biology and medical diagnostics for the cell sample preparation, "Centrifuge-on-a-chip" benefits from its small footprint, ability to treat small volume and rare cell sample, high concentration capacity, and multifunctional character (e.g. concentrate and sequentially treat cells with chemical, biological agents to reduce human miscellaneous and toilsome operation and its consequent error) [1].

Shelby *et al*. [2-4] were the first to propose the application of micro-vortex generated within a diamond-shaped microchamber on the field of microfluidics, investigating the effects of high radial acceleration on biological and chemical processes. They also analyzed the formation mechanism of colloidal particles' ring-shaped patterns [5]. The formation relies on the balance of two outward inertial forces (centrifugal and displacement forces) and one inward hydrodynamic force (wall lift force). Additionally, in order to address the lack of techniques to characterize the rotation of single micro-particle, they proposed two methods to mark and monitor rotational behavior of optically trapped single micro-particle and living cell, respectively. For polystyrene beads, a single nanosecond pulse from a UV laser was used to ablate a small area on its surface as a mark, and its rotation was tracked by recording changes in the level of backscattered light. For the biological cells, a fluorescence dye was selectively stained to a portion of the cell, and rotation could be observed by monitoring changes in the fluorescence signal [6]. It should be noted that the trapping and positioning of micro-particles in the micro-vortex core here was achieved by a Nd:YAG laser.

Later, Di Carlo *et al.* [1, 7] introduced the concept of "Centrifuge-on-a-chip" to isolate rare cells from heterogeneous blood sample. The functions of trapping, enrichment, labeling and solution exchange were also proven by the experiments. Other than the optical laser, the selective trapping and positioning of micro-particles in "Centrifuge-on-a-chip" were based on purely fluid dynamic phenomenon: the inertial migration of micro-particles in the cavity expanding area. The most significant advantage of "Centrifuge-on-a-chip" is its ability to selectively trap particles from mainstream according to particle size. For example, rare cancer cells can be trapped from heterogenerous blood sample, and this can be then followed by the enumeration in the downstream for the diagnostics of metastatic cancer [8].

The mechanism of trapping has been qualitatively explained by Mach *et al.* [1]. Briefly, the particle trapping process, as shown in Fig. 1, is divided into three steps: (i) focusing in the straight channel section; (ii) lateral migration in the expanding area; and (iii) circulation within micro-vortex.

(i) In the straight channel section, particles begin uniformly distributed across the channel cross-section when particles suspension is introduced into the micro-channel. As they are travelling downstream, they will suffer a shear gradient lift force F_{LS} and a wall effect lift force F_{LW}, which compete against each other in the lateral direction. The final result is that one or more equilibrium positions of particles appear. This phenomenon was first observed experimentally by Segre & Silberberg [9]. Later, a series of theoretical and experimental studies were conducted [10-16]. Based on the technique of matched asymptotic expansions, the net lift force F_L of shear gradient lift force and wall lift force can be scaled as: $F_L = f_L \rho_f U_m^2 d^2 / D_h^2$, where f_L is a non-dimensional lift coefficient. ρ_f is density of fluid. U_m is maximum velocity of fluid. d is diameter of particles. D_h is hydraulic diameter of channel, defined as $D_h = D$ for a circular channel (D is the diameter of circular cross section) and $D_h = 2wh/(w+h)$ for a rectangular channel (w and h correspond to the width and height of rectangular cross-section) [14, 17-18]. However, the expression of shear gradient lift force and wall lift force are hard to obtain as they are always complexly coupled in the real situation.

(ii) When the focused particles reach the suddenly expansion-contraction area, the adjacent micro-channel wall

All Authors are with School of Mechanical, Materials and Mechatronic Engineering, University of Wollongong, Wollongong, NSW 2522, Australia (corresponding author e-mail: weihuali@uow.edu.au).

is out of its vicinity. Therefore, the wall lift force on the particles which is the result of hydrodynamic interaction between particles and walls disappears. The shear gradient lift force will solely act on the particles, leading particles to migrate across streamlines towards the vortex. The shear gradient, which is responsible for the shear gradient lift force, decays slowly in the expanding area [1]. The lateral migration velocity v_t can be determined by the balance of the shear gradient lift force and Stokes drag $F_{stk} = 3\pi\mu_f d v_t$ where μ_f is dynamic viscosity of fluid. From the analytical scaling by Di Carlo *et al.* [16], shear gradient lift force is scaled as: $F_{LS} \sim \rho_f U_m^2 d^3 / D_h$. Then lateral migration velocity is scaled as: $v_t \sim U_m^2 d^2 / D_h$. It indicates that lateral migration velocity of particles is proportional to the square of particle diameter. So it can be expected that larger particles will migrate much faster than smaller ones. Larger particles with higher lateral migration speed are possible to cross the streamlines into the vortex, while smaller particles below a critical size can't enter the vortex. It should be noted that entry into the vortex is controlled solely by shear gradient lift forces in the case of a dilute particles solution where particle-particle interactions can be neglected. For a highly concentrated particles solution, such as blood sample, the cross-stream migration and entry can be assisted by particle collisions or disturbance flows from nearby particles.

(iii) After particles enter into the micro-vortex, the issue of maintaining particles in vortex becomes important. As the shear gradient still exists in the micro-vortex, the relevant shear gradient lift F_{LS} should still act on the micro-particles, directing towards the vortex centre. However, this shear gradient lift force is rather difficult to be expressed explicitly by shear rate, because flow field is more complex in the expansion-contraction area than that in a straight channel [1].

As mentioned above, the shear gradient lift force is supposed to dominate the particles' lateral migration in the expanding area, then determines the selective trapping of particles from main stream. However, due to the lack of its explicit expression, the accurate mechanism of migration process and selective trapping is still unclear, which limits the application of "Centrifuge-on-a-chip" on the practical diagnostics. In this paper, we firstly derived an explicit expression of shear gradient lift force based on the work of Asmolov [14] and a linear assumption. Then, a computational fluid dynamic (CFD) code was developed to predict the trajectories of particles in the expanding area. Finally, microfluidic chip and experimental setups were fabricated and developed to verify trapping process of particles in the cavity area. The effects of flow condition and particle size on the particle trapping process were also studied.

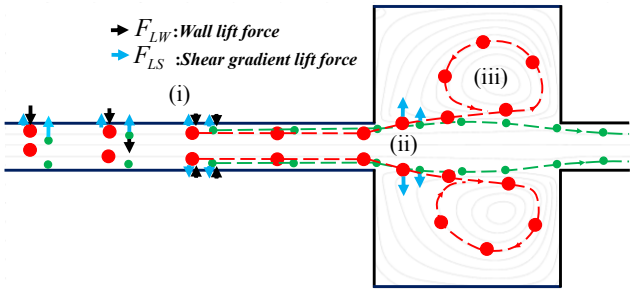

Figure 1. Three steps of particles' trapping process in a "Centrifuge-on-a-chip": (i) Particles focusing in the straight channel. (ii) lateral migration in the expanding area. (iii) Circulation within micro-vortex.

II. DERIVATION OF SHEAR GRADIENT LIFT FORCE

The inertial lift force is divided into two parts: shear gradient lift force and wall lift force. In the expanding area, shear gradient lift force dominates particles' lateral migration due to the disappearance of adjacent walls and its consequent wall lift force [1]. Shear gradient lift force is generated by the curvature of parabolic velocity profile in a pipe flow. Asmolov [14] employed matched asymptotic expansions method to solve the equations governing the movement of neutrally buoyant spheres in a unbounded parabolic flow. The shear gradient lift force can be expressed as:

$$F_{LS} = f_{LS} \rho_f G^2 d^4 \tag{1}$$

where G is local shear rate at particle centre. f_{LS} is shear gradient lift coefficient, and it has been solved by the numerical method.

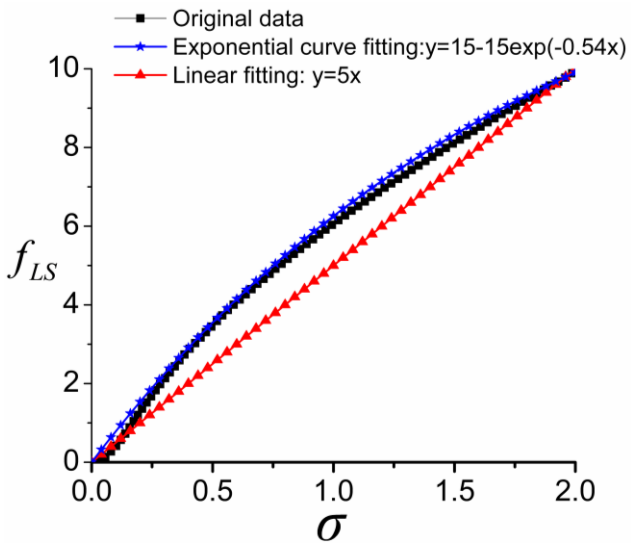

Figure 2. Lift coefficient for a neutrally buoyant particle in unbounded poiseuille flow.

For simplicity, we consider the situation where particles suspension is moving in a circular channel, so that three dimensional question is now simplified to a 2-dimensional problem. From Fig. 2, it indicates that the shear gradient lift

coefficient increases monotonically with parameters σ, ($\sigma = (x/R)^{-3/2} R_C^{-1/2}/2$) [14], where x is distance between particle center and the symmetry axis of circular channel. R is radius of the circular channel. R_C is channel Reynolds number, $R_C = \rho_f U_m D/\mu_f$, where U_m is maximum velocity of fluid in the channel and D is diameter of circular channel. In order to obtain an analytical expression of shear gradient lift coefficient, two different fitting methods have been used: (1) linear fitting; and (2) exponential curve fitting. The results are plotted in Fig. 2. We can see that exponential curve fitting is much closer to the original data than linear fitting. However, the expression of exponential curve fitting is still too complex to get an explicit and simple expression for the shear gradient lift force. In this paper, we select a linear fitting for simplicity:

$$f_{LS} = 5\sigma = 2.5(x/R)^{-3/2} R_C^{-1/2} \tag{2}$$

As

$$G = 2xU_m/R^2 \tag{3}$$

$$U_m = 1.5U_f \tag{4}$$

where U_f is fluid average velocity [19].

Then shear gradient lift force is:

$$F_{LS} \cong 13\mu_f^{1/2}\rho_f^{1/2}U_f^{3/2}d^4x^{1/2}/R^3 \tag{5}$$

In (2), the shear gradient lift coefficient f_{LS} is infinite when particle is at the centerline of the channel $x = 0$, as shown in Fig. 3. But as we know, the shear gradient lift force is zero at the centerline of channel due to its symmetrical characteristics in a rectangular or circular channel [14, 20]. Meanwhile, f_{LS} decreases sharply as the distance ratio x/R increases and approximates to $2.5R_C^{-1/2}$ at the channel walls, which is also opposite to the actual trend of shear gradient lift force F_{LS}. This shear gradient lift coefficient f_{LS} is not consistent with its shear gradient lift force F_{LS}, which might bring conflicts and confusions in the analysis. We derived a new shear gradient lift coefficient f_{LS2} (as shown in (6)) to overcome these problems. Its relationship with particle lateral position within the cross section of channel was shown in Fig. 3(b).

$$f_{LS2} = 13(x/R)^{1/2} \tag{6}$$

$$F_{LS} = f_{LS2}\mu_f^{1/2}\rho_f^{1/2}U_f^{3/2}d^4/R^{5/2} \tag{7}$$

It can be concluded that this new shear gradient lift coefficient f_{LS2} accords quite well with the shear gradient lift force at least in two aspects. One is that its value is zero at the centerline $x/R = 0$, which is consistent with shear gradient lift force. Because shear rate is zero at the centerline of channel due to its symmetrical characteristics, and shear gradient lift force is generated just due to the non-zero shear rate and its gradient. The other is that its trend with distance ratio x/R, that f_{LS2} increases with the distance ratio and reaches the maximum value at the channel surface, is accordant with the shear gradient lift force as shear rate reaches maximum at the walls of channel. So it can be concluded that this new shear gradient lift coefficient f_{LS2} can characterize shear gradient lift force in a more reasonable way.

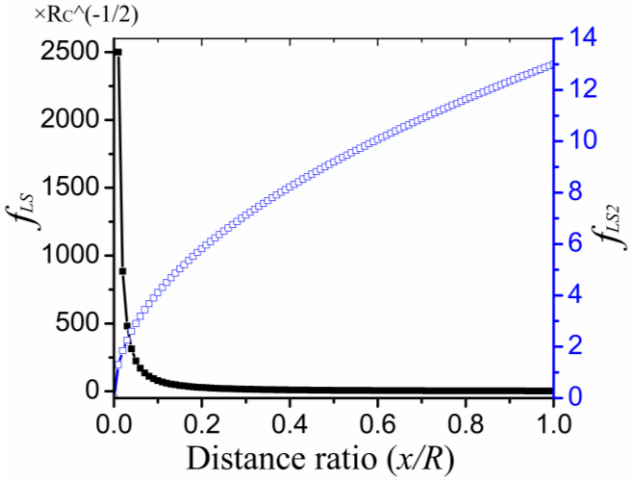

Figure 3. The lift coefficient f_{LS} decreases with the distance ratio x/R, and approximates to $2.5R_C^{-1/2}$ at channel surface (left). The new lift coefficient f_{LS2} increases with the distance ratio, and reaches maximum value at the channel surface (right).

III. NUMERICAL MODELLING

A numerical modeling was developed to predict particles' lateral migration in the expansion-contraction area. The numerical simulation can support analysis of separation or trapping, and instruct the design of "Centrifuge-on-a-chip". As the concentration of particle suspension is very low, the interaction of particles can be neglected. Thus, the particles experience four kinds of forces when passing the expansion-contraction area: shear gradient lift force, drag force, buoyancy force and gravity. Based on Newton's second law of motion, we can get:

$$m_P \frac{d^2\vec{X}}{dt^2} = \vec{F}_{LS} + \vec{F}_{drag} + \vec{F}_{buoyancy} + \vec{F}_{gravity} \tag{8}$$

$$m_P = \rho_P \pi d^3/6 \tag{9}$$

where ρ_P, m_P and $\vec{X}$ are particle density, mass and position vector, respectively.

In a normal situation, microfluidic chip is placed parallel to the surface of earth, and particles' motion in horizontal plane is considered as independent of the forces in vertical direction, also the density of polymer particle is almost equal to the solution. Equation (8) can be further simplified by neglecting the effects of buoyancy and gravity, as following:

$$m_P \frac{d^2\vec{X}}{dt^2} = \vec{F}_{LS} + \vec{F}_{drag} \tag{10}$$

Stokes drag law is used to calculate the drag of particles' migration in fluid:

$$\vec{F}_{drag} = 3\pi\mu_f d(\vec{v} - \vec{v}_P) \quad (11)$$

where $\vec{v}$ and $\vec{v}_P$ are velocity vector of fluid and particles, respectively. Equation (7) is used for the calculation of shear gradient lift force. The ordinary differential equation (10) is solved by a pair of runge-kutta methods of orders four and five.

In our study, laminar steady incompressible flow model is applied to calculate the flow field in the micro-channel, as flow Reynolds number is much lower than 2000 in the micro-channel, and liquid solution filled within the micro-channel is incompressible. Equations governing steady incompressible flow are:

Steady N-S equation:

$$\rho_f \vec{v} \cdot \nabla \vec{v} = -\nabla P + \mu_f \nabla^2 \vec{v} \quad (12)$$

Continuity equation:

$$\nabla \cdot \vec{v} = 0 \quad (13)$$

Non-slip boundary condition:

$$\vec{v}_w = 0 \quad (14)$$

where $\vec{v}$ and P are the velocity vector and pressure of fluid, respectively; $\vec{v}_w$ is fluid velocity vector at the channel walls. The inlet condition is an input fluid velocity v_{in} which is uniform at the inlet, and equal to average fluid velocity U_f. The flow field is calculated using software of COMSOL Multiphysics@ (COMSOL, Burlington, MA) that solves the partial differential equations (PDEs) by finite element methods. The overall flowchart of calculation is shown in the Fig. 4.

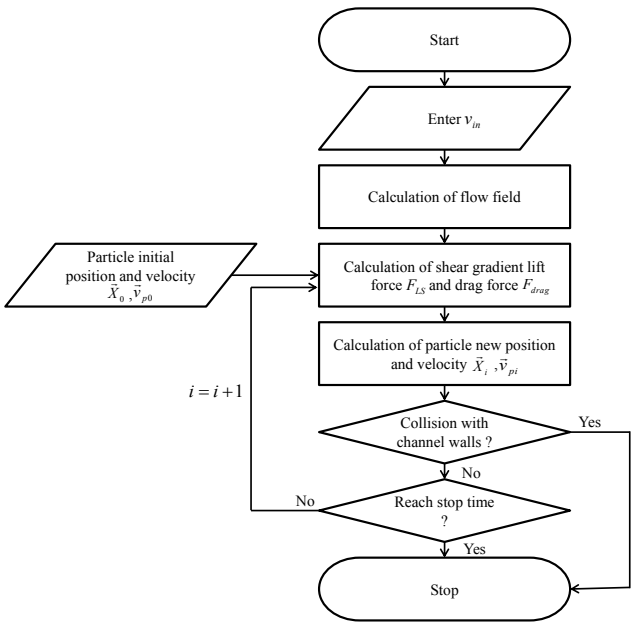

Figure 4. Flowchart for the calculation of particles' trajectory in the process of inertial migration in the expansion-contraction area.

IV. FABRICATION AND EXPERIMENTAL SETUP

A. Design and fabrication of a microfluidic device

The aspect ratio of the straight channel is 1.4, with a cross-section of 50 μm×70 μm (width × height). The length of first straight section is $L_1 = 10mm$, allowing enough path for the uniformly distributed particles reaching their inertial equilibrium position before arriving at expansion-contraction area [1, 18]. The dimension of rectangular cavity is $W = 275\mu m$, $L = 900\mu m$. The space between each rectangular cavity is uniform as $L_2 = 900\mu m$. Its schematic geometry is shown in Fig. 5(a). The device was fabricated by the standard photolithography and soft lithography techniques which typically included three steps: rapid prototyping of a silicon master, polydimethylsiloxane (PDMS) replica molding, and sealing.

B. Experimental setup

Particles suspension was shaken vigorously before being transferred to a 5ml syringe, and then introduced into the microfluidic chip through a silicon tube by a syringe pump (Legato 100, Kd Scientific). The microfluidic chip was placed in an inverted microscope (CKX41, Olympus, Japan), illuminated by a mercury arc lamp. The fluorescence images of fluorescent particles were observed and captured by a CCD camera (Rolera Bolt, Q-imaging, Australia). The fluorescence images were then post-processed and analysed in the software Q-Capture Pro 7 (Q-imaging, Australia). The exposure time for each frame was uniform as 100 ms. The schematic diagram of experimental setup is shown in Fig. 5(b).

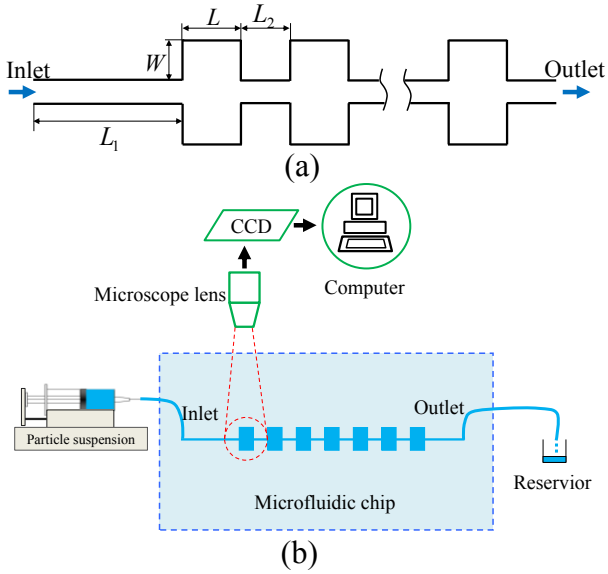

Figure 5. (a) Geometry of micro-channel with rectangular expansion-contraction cavity. (b) Schematic illustration of the experimental setup.

V. RESULTS AND DISCUSSION

A. Effects of flow condition

The flow condition dominates the flow field in the cavity, thereby controls the trapping process of particles in the cavity area. The 9.9 μm particles' trajectory was calculated by the proposed modeling with and without the consideration of shear gradient lift force respectively, and then compared with the experimental ones, as shown in Fig. 6.

Generally speaking, the calculated particle trajectory with the consideration of shear gradient lift force agrees more closely with the experimental trajectory, especially at larger channel Reynolds number R_C. At $R_C = 218.8$, the model with the consideration of shear gradient lift force can perfectly predict the trapping of particles into the vortex which coincides quite well with the experimental ones, whereas the model without consideration of shear gradient lift force can't predict it. It indicates that the shear gradient lift force actually exists in the sudden expanding area.

At small R_C, particles can't migrate laterally into the vortex although vortex is already developed partially in the cavity. It can be explained by the fact that the shear gradient lift force is quite small at low flow rate, leading to not enough lateral migration distance. From (5), we get $F_{LS} \sim U_f^{3/2}$, then lateral migration velocity $v_t \sim U_f^{1.5}$. The duration for the particles passing through the cavity area is: $t \sim 1/U_f$, so the lateral migration distance before particles pass through the cavity is $l = v_t * t \sim U_f^{1/2}$ .It means that lateral migration distance will increase with the increasing input velocity even though the duration for particles in the expansion-contraction area decreases. So the trapping of particles in vortex happens after flow rate (or channel Reynolds number) exceeds a certain level, generally after a fully developed vortex is created.

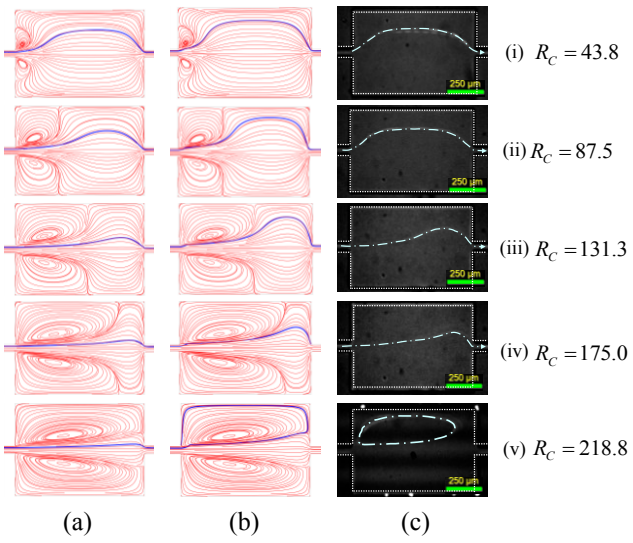

Figure 6. The trajectory of 9.9 μm particles under different flow conditions by simulation and experiments. (a) Simulation results without consideration of shear gradient lift force. (b) Simulation results with consideration of shear gradient lift force. (c) Experimental results.

B. Effects of particle size

As mentioned above, particles can be selectively trapped into the vortex according to their sizes. From (5), the shear gradient lift force F_{LS} is proportional to d^4, so we can expect that particles with larger diameter experience bigger shear gradient lift force, leading to higher lateral migration velocity. In the same duration, particles with a diameter larger than a critical size can transfer into the vortex. The trajectory of particles with diameters of 5 μm, 10 μm, 12 μm, 14 μm, 16 μm were calculated, and compared with the experimental results from Mach *et al.* [1], as shown in Fig. 7. It indicates that larger particles can be trapped, while particles smaller than 10 μm can't migrate into vortex. Furthermore, larger particles migrate into more inner side of vortex. The trend of predicted trajectory agrees well with the experimental ones. However, the predicted trajectory is mostly on the outer side of experimental ones, except that of 5 μm particles which agrees perfectly with experimental one. The error could be due to the expression of shear gradient lift force that was derived based on the assumption of linearity and channel with circular cross section. And also that the effects of shear gradient on the particles within the vortex was ignored in the simulation due to its unclear mechanism, and it could be another major error source [1].

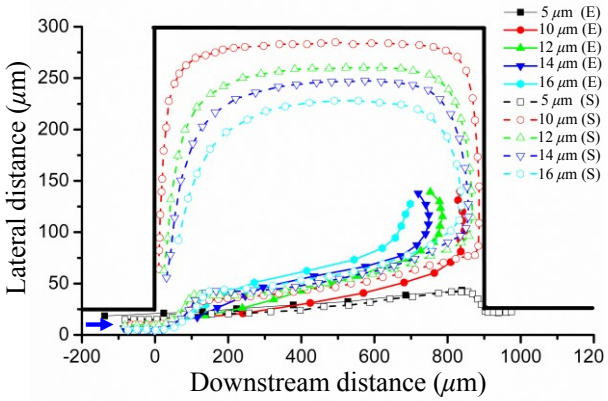

Figure 7. The trapping trajectory of particles with different sizes. The solid line with symbol (E) is the experimental data from Mach *et al.* [1], and dashed line with symbol (S) is the simulation results calculated by the proposed model.

VI. CONCLUSION

This paper is focused on the selective trapping ability of "Centrifuge-on-a-chip". The mechanism of the selective trapping was studied by both the numerical modeling and experiments. The expression of shear gradient lift force which dominates the lateral migration of particles in the expansion-contraction cavity was derived based on a linear assumption. A numerical modeling was developed successfully to predict the lateral migration of particles. The effects of flow condition and particle size on the trapping process were investigated. It can be concluded that the derived expression and developed numerical modeling are suitable for the prediction of particles' trapping process, which is useful for the design of "Centrifuge-on-a-chip".

REFERENCES

[1] A. J. Mach*, et al.*, "Automated cellular sample preparation using a Centrifuge-on-a-Chip," *Lab on a Chip,* vol. 11, pp. 2827-2834, 2011.

[2] J. P. Shelby*, et al.*, "Microfluidic systems: high radial acceleration in microvortices," *Nature,* vol. 425, pp. 38-38, 2003.

[3] J. P. Shelby and D. T. Chiu, "Controlled rotation of biological micro-and nano-particles in microvortices," *Lab Chip,* vol. 4, pp. 168-170, 2004.

[4] D. T. Chiu, "Cellular manipulations in microvortices," *Analytical and bioanalytical chemistry,* vol. 387, pp. 17-20, 2007.

[5] D. S. W. Lim*, et al.*, "Dynamic formation of ring-shaped patterns of colloidal particles in microfluidic systems," *Applied Physics Letters,* vol. 83, pp. 1145-1147, 2003.

[6] J. P. Shelby*, et al.*, "Direct manipulation and observation of the rotational motion of single optically trapped microparticles and biological cells in microvortices," *Analytical Chemistry,* vol. 76, pp. 2492-2497, 2004.

[7] S. C. Hur*, et al.*, "High-throughput size-based rare cell enrichment using microscale vortices," *Biomicrofluidics,* vol. 5, p. 022206, 2011.

[8] M. Cristofanilli*, et al.*, "Circulating tumor cells, disease progression, and survival in metastatic breast cancer," *New England Journal of Medicine,* vol. 351, pp. 781-791, 2004.

[9] G. Segre, "Radial particle displacements in Poiseuille flow of suspensions," *Nature,* vol. 189, pp. 209-210, 1961.

[10] P. G. Saffman, "The lift on a small sphere in a slow shear flow," *Journal of Fluid Mechanics,* vol. 22, pp. 385-400, 1965.

[11] P. Vasseur and R. G. Cox, "The lateral migration of spherical particles sedimenting in a stagnant bounded fluid," *Journal of Fluid Mechanics,* vol. 80, pp. 561-591, 1977.

[12] J. A. Schonberg and E. J. Hinch, "Inertial migration of a sphere in Poiseuille flow," *Journal of Fluid Mechanics,* vol. 203, pp. 517-524, 1989.

[13] J. B. McLaughlin, "Inertial migration of a small sphere in linear shear flows," *Journal of Fluid Mechanics,* vol. 224, pp. 261-274, 1991.

[14] E. S. ASMOLOV, "The inertial lift on a spherical particle in a plane Poiseuille flow at large channel Reynolds number," *Journal of Fluid Mechanics,* vol. 381, pp. 63-87, 1999.

[15] J.-P. MATAS*, et al.*, "Inertial migration of rigid spherical particles in Poiseuille flow," *Journal of Fluid Mechanics,* vol. 515, pp. 171-195, 2004.

[16] D. Di Carlo*, et al.*, "Particle segregation and dynamics in confined flows," *Physical review letters,* vol. 102, p. 94503, 2009.

[17] A. A. S. Bhagat*, et al.*, "Enhanced particle filtration in straight microchannels using shear-modulated inertial migration," *Physics of Fluids,* vol. 20, p. 101702, 2008.

[18] D. Di Carlo, "Inertial microfluidics," *Lab on a Chip,* vol. 9, pp. 3038-3046, 2009.

[19] J. M. Martel and M. Toner, "Inertial focusing dynamics in spiral microchannels," *Physics of Fluids,* vol. 24, p. 032001, 2012.

[20] J. P. Matas*, et al.*, "Lateral force on a rigid sphere in large-inertia laminar pipe flow," *Journal of Fluid Mechanics,* vol. 621, p. 59, 2010.